

# Energy Dissipation and Mechanoresponsive Color Evaluation of a Poly(*n*-hexyl Methacrylate) Soft Material Enhanced by a Mechanochromic Cross-Linker with Dynamic Covalent Bonds

Yuchen Mao, Yuto Kubota, Takashi Kurose, Akira Ishigami, Kota Seshimo, Daisuke Aoki, Hideyuki Otsuka, and Hiroshi Ito\*



Cite This: <https://dx.doi.org/10.1021/acs.macromol.0c01770>



Read Online

ACCESS |



Metrics & More

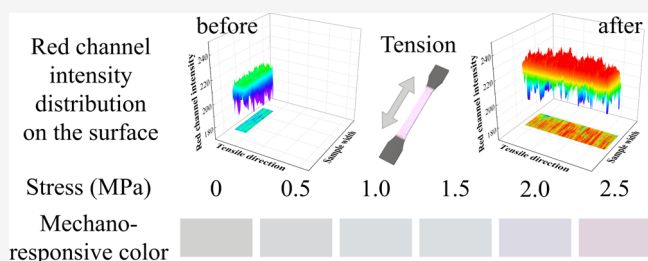


Article Recommendations



Supporting Information

**ABSTRACT:** A rigid and brittle cross-linking structure was introduced into the flexible poly(*n*-hexyl methacrylate) (PHMA) network by the mechanochromic cross-linker difluorenylsuccinonitrile-containing methacrylate (DFMA), whose central C–C bond acted as a dynamic covalent bond and could generate pink radicals when fractured. PHMA with DFMA showed a remarkable hysteresis loop and mechanical enhancement. After deformation, the reassociation of dynamic covalent bonds and the reorganization of the network structure slowed down the recovery of the polymer to its initial state. The correlations between tension stimulation, energy dissipation, and mechanoresponsive color change were discussed. Under stress, the polymer changed from light gray to pink. The broad distribution of red channel intensity under large deformation detected on the surface confirmed that the rupture of dynamic covalent bonds occurred evenly throughout the polymer and suppressed stress concentration. The color showed a strong dependence on stress, which started to appear at around 1.5 to 2.0 MPa. The incorporation of DFMA promised mechanical enhancement and noncontact stress detection ability of the PHMA soft material.



## 1. INTRODUCTION

Many biomass materials, such as spider silk, nacre, mussel byssus, and bones, are well known for their extraordinary strength and toughness, as well as outstanding self-healing ability.<sup>1–3</sup> Dynamic covalent bonds, which often act as sacrificial bonds, are the key factors contributing to the excellent mechanical enhancement. When a load is applied, sacrificial bonds can rupture before the fracture of the main skeleton, dissipating a large amount of energy and enhancing strength greatly. Meanwhile, the released hidden lengths that are constrained from stretching by sacrificial bonds will dramatically improve toughness and increase elongation.<sup>4–6</sup> Hydrogen bonds, metal–ligand coordination bonds, and ionic bonds are common sacrificial bonds.<sup>7–10</sup>

Inspired by this concept, studies have shown that significant mechanical enhancement, such as stiffness, strength, toughness, fatigue resistance, and self-healing, can be realized by incorporating dynamic covalent bonds into matrix materials.<sup>2,11,12</sup> Gong et al.<sup>7,13,14</sup> developed a high-toughness double-network hydrogel consisting of a rigid and brittle first network as sacrificial bonds and a soft and flexible second network. The internal fracture of the first network dissipated the amount of energy during stretching, while the elasticity of the second network allowed the material to return to its initial state.<sup>14</sup> However, because of the permanent damage caused by the ruptured first network, this material could not fully recover

after experiencing a large deformation. By introducing the sacrificial bonds with the reversibility, materials will present self-repairing after releasing the load. Guan et al.<sup>8</sup> incorporated dynamic hydrogen bonds into a self-repairable network. The material showed a great energy dissipation capacity and self-healing ability. Constructing dynamic covalent bonds in the chemical structure of soft polymer materials, including gels and elastomers, can be exploited to enhance their mechanical performance.

Mechanochromic polymers, which change color responding to mechanical stimulations, have attracted much attention because they can detect damage and stress on a material, enabling it to be replaced or repaired before failure.<sup>15–24</sup> Related research studies provided insights into the action–reaction relationships of polymers and their composites under external force application and subsequent deformation. Sottos et al.<sup>20</sup> discussed fracture-induced mechanochemical activation along the crack during single-edge notch tensile tests on a

Received: July 29, 2020

Revised: October 6, 2020

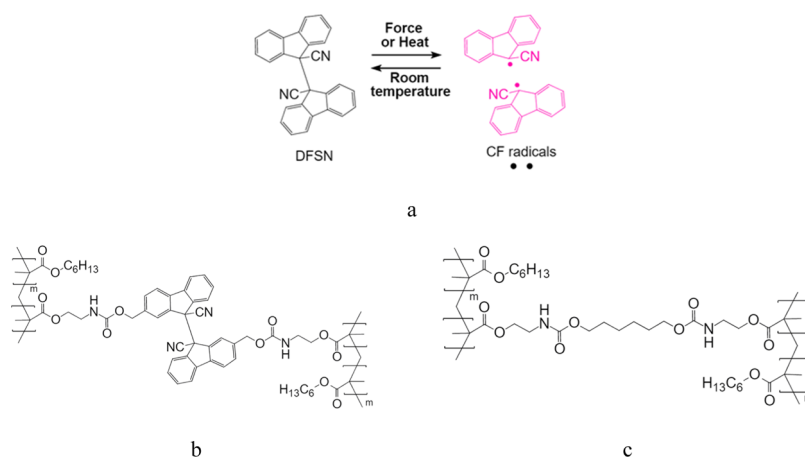


**Figure 1.** Equilibrium between DFSN and its pink-colored CF radical species (a), chemical structure of the PHMA polymer network cross-linked by the mechanochromic cross-linker DFMA (b) and the conventional cross-linker HDMA (c).<sup>19,41,42</sup>

spiropyran-linked material. Owing to the advantages of high resolution and efficacy to pinpoint the exact location site of crack propagation, with the aid of fluorescence microscopy, mechanophore activation had the potential for damage sensing in glassy bulk polymers and as an indicator of plastic deformation.<sup>20–22</sup> Zheng et al.<sup>6</sup> developed a multistimuli-responsive hydrogel cross-linked by spiropyran. The material exhibited thermo-, photo-, and mechanoresponsive color changes and reversed its color by exposure to white light for about 30 min. We have reported a class of mechanochromic molecules, such as diarylbibenzofuranone,<sup>25–34</sup> tetraarylsuccinonitrile,<sup>32,35–39</sup> diarylbibenzothiophenonyl,<sup>32,36</sup> diarylbiindolinone,<sup>40</sup> and difluorenylsuccinonitrile (DFSN),<sup>41,42</sup> whose central C–C bonds are weaker than conventional covalent bonds and easier to rupture under stress. The fractures of the central C–C bonds occur homolytically and generate relatively stable pink-colored cyanofluorenyl (CF) radicals,<sup>41,42</sup> the equilibrium shown in Figure 1a. DFSN-containing dimethacrylate (DFMA) is a mechanochromic cross-linker with vinyl groups, which have reactivity to form a polymer with the aid of a radical initiator.<sup>41,42</sup> The generated reversible and detectable pink color under stress provides a promising way for the quantitative evaluation of energy dissipation from a visual perspective. Establishing the correlation between macroscopic mechanical stimulations and molecular-scale mechanophore activation, including structural transition and energy dissipation, helps us to get a better understanding of mechanochromic polymers with detectable optical signals.<sup>15,18–21,40</sup>

In this paper, under tension stimulation, the energy dissipation and mechanoresponsive color evaluation of the soft material enhanced by dynamic covalent bonds were systematically investigated. The toughening poly(*n*-hexyl methacrylate) (PHMA) network with 1 wt % DFMA was synthesized through radical polymerization, as the previous report.<sup>19,41,42</sup> For comparison, the conventional cross-linker hexamethylene-containing dimethacrylate (HDMA) with the same concentration was used to prepare the polymer as a control. The chemical structures of PHMA with DFMA and HDMA are shown in Figure 1b,c, respectively. Continuous uniaxial loading–unloading cycles were measured for hysteresis analysis. The dissociation and reassociation of dynamic covalent bonds and structure transition of the polymer network under stress were discussed. With the aid of digital image analysis, the generated reversible pink color was quantitatively

evaluated. By investigating the three primary color (RGB) channel intensities, we explored the correlations between tension stimulation, energy dissipation, and mechanoresponsive color change in the stretching–relaxation process. The study on mechanoresponsive color changes of mechanochromic soft polymer materials induced by structural transition under stress provided a new pathway for quantitative evaluation of energy dissipation from a visual perspective.

## 2. METHODS

**2.1. Tensile Test and Energy Dissipation Analysis.** Uniaxial tensile tests were performed on a STROGRAPH VGS1-E vertical tension testing machine (Toyo Seiki Seisaku-Sho Ltd., Tokyo, Japan) with a dumbbell-shaped sample standardized to JIS-7. PHMA cross-linked by DFMA and HDMA was measured under a load of 10 N at room temperature with a solid testing rate of 20 mm/min. Three sets of tests with different conditions were conducted to evaluate the mechanical performance and energy dissipation.

In hysteresis analysis, the sample was first stretched to a certain strain and then unloaded. After the stress relieved, the sample was stretched to the same strain again immediately. The energy dissipation and shape recovery in two testing cycles were recorded. The strains ranged from 25% to break.

Continuous loading–unloading cycles of PHMA soft materials with increasing deformation were measured to investigate the dissociation and reassociation of the central C–C bonds of DFMA. After the first cycle with a strain of 25%, the sample was stretched to a strain of 50% for the next cycle immediately. Without relaxation, this process was repeated with increasing deformation until a break.

To further evaluate the energy dissipation of dynamic covalent bonds and the recovery ability of PHMA, the stretching–relaxation process with different time intervals was measured. The sample was stretched to a strain of 600% and then unloading immediately. After relaxation at room temperature for a certain time, including 0 min, 0.5 min, 1 min, 2 min, 5 min, 10 min, 30 min, 60 min, and 120 min, the loading–unloading cycles to the same strain were repeated.

The tension energy ( $W_t$ ) was defined as the area surrounded by the stress–strain curves during loading. The integrated area of the hysteresis loop during one loading–unloading cycle was calculated as dissipated energy ( $W_d$ ).

$$W_t = \int_{\text{loading}} \sigma \, d\varepsilon \quad (1)$$

$$W_d = \int_{\text{loading}} \sigma \, d\varepsilon - \int_{\text{unloading}} \sigma \, d\varepsilon \quad (2)$$

where  $\sigma$  is the stress (MPa) and  $\varepsilon$  is the strain (%). The yield stress was determined based on the Considère criterion analysis.<sup>43,44</sup> The

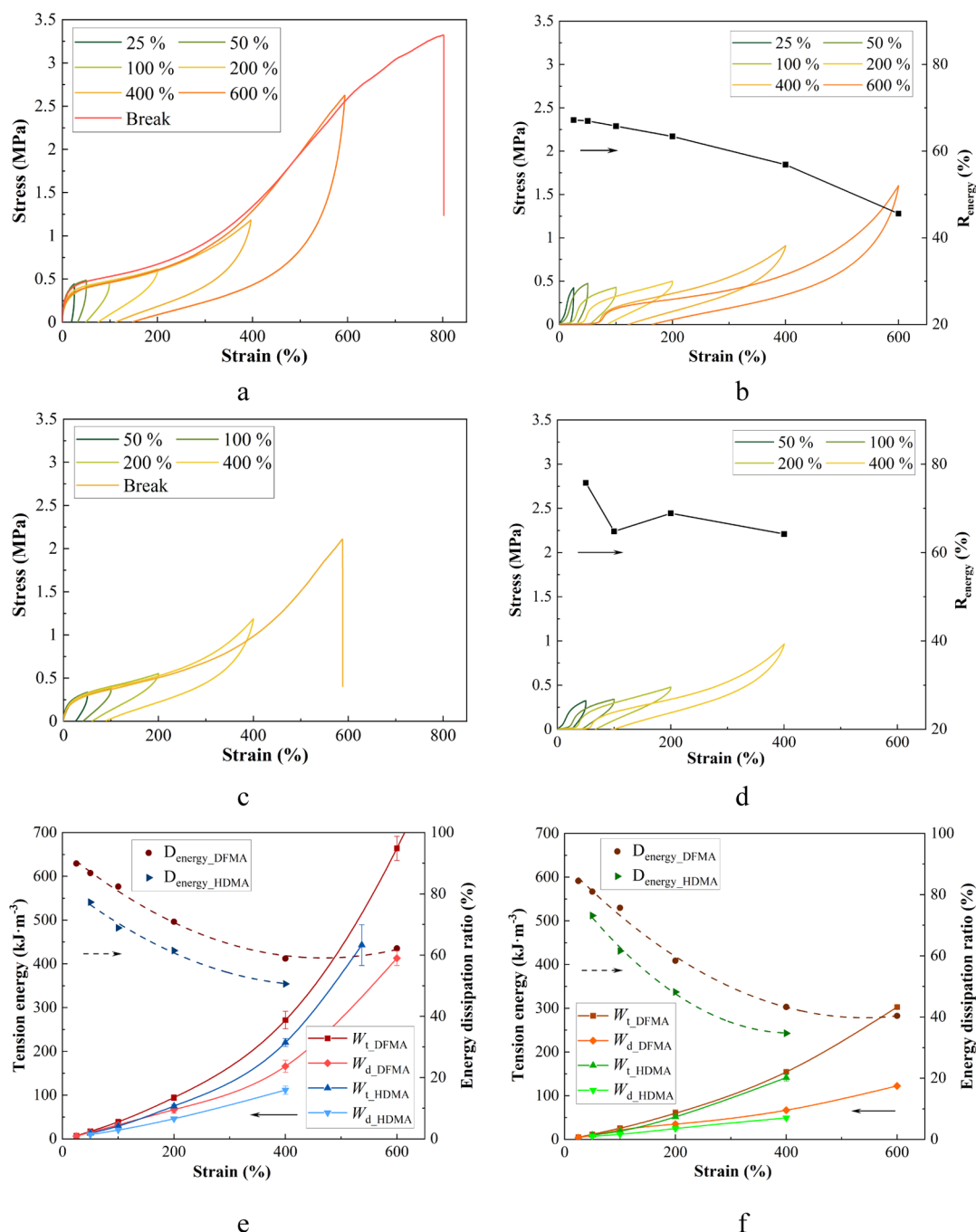


**Figure 2.** Stress–strain curves of PHMA with DFMA (a,b) and HDMA (c,d) in the first and second loading–unloading cycles, and the comparisons of energy dissipation in two cycles (e,f).  $R_{\text{energy}}$ : energy recovery ability,  $R_{\text{energy}} = W_{\text{t\_cyc2}}/W_{\text{t\_cyc1}}$ ,  $D_{\text{energy}}$ : energy dissipation ratio, and  $D_{\text{energy}} = W_{\text{d}}/W_{\text{t}}$ .

yield point was the tangent point by making a tangent to the stress–strain curve at  $\varepsilon = -1$ . All data were calculated via OriginPro 2020b (OriginLab Corp., Northampton, USA).

**2.2. Digital Image Analysis.** Under stress, PHMA cross-linked by DFMA generated reversible and detectable pink CF radicals. With the aid of digital image analysis, the correlations between tension stimulation, energy dissipation, and mechanoresponsive color change during the stretching–relaxation process were discussed. By analyzing the three primary color (RGB: red, green, and blue) channel intensities and distributions, it allowed us to quantitatively evaluate the dissociation and reassociation of dynamic covalent bonds, as well as energy dissipation, from a visual perspective.

An LCD monitor (Brilliance 288P, Philips, Tokyo, Japan) was set to a blank as a surface light source. The digital images in loading–

unloading cycles were taken by the Canon EOS Kiss X8i camera (Canon Inc., Tokyo, Japan), which was remote controlled via EOS Utility and Digital Photo Professional 4 software (Canon Inc., Tokyo, Japan). All images with a white background were white-balanced first via ImageJ software (National Institute of Health, USA). The white background reached the RGB value of (220, 220, 220) after image processing. Then, the RGB channel intensities of samples on the surface were extracted from digital images via ImageJ. 3D color maps of red channel intensity distributions and fitting curves were plotted via OriginPro 2020b. The red channel intensities on the central axis of the tensile direction were also shown. The simulated colors were obtained based on the fitting results of average RGB values on the surface and referred to the color book provided by <https://www.colortell.com> (ColorTell Tech Co., Ltd., Beijing, China).

### 3. RESULTS AND DISCUSSION

**3.1. Hysteresis Analysis in Loading–Unloading Cycles.** The mechanical properties of polymer materials are strongly affected by the flexibility of the polymer network. The segment mobility, crystallinity, orientation of the molecular chain, and cross-linking density have strong effects on the mechanical properties. In this study, the dissociation and reassociation of dynamic covalent bonds is a key element for toughening and energy dissipation. The stress–strain curves of PHMA in the first and second loading–unloading cycles are shown in Figure 2a–d, and related data are summarized in Tables S1 and S2. The comparisons of energy dissipation in two cycles are summarized in Figure 2e,f, respectively. PHMA samples with both the mechanochromic cross-linker DFMA and the conventional cross-linker HDMA had notable hysteresis loops. The soft polymer showed a higher energy dissipation capacity with increasing deformation. Because of the low glass transition temperature of PHMA (around 0 °C)<sup>42</sup> and a relatively low cross-linking density, the polymer network was in a high-elastic state with great segment mobility and poor deformation resistance at room temperature. The intermolecular entanglements and rearrangement of the main skeleton in stretching caused the large hysteresis loops.

Compared to PHMA cross-linked by HDMA, the introduction of DFMA promised mechanical enhancement with no decline in toughness and elongation. The breaking stress of the toughening polymer was up to 3.29 MPa that was 1.5 times higher than that of PHMA cross-linked by HDMA, with a fracture energy of 1278.1 kJ·m<sup>-3</sup> increased by 289%, while the maximum elongation at break reaching 810.2% increased by 151%. Under stress, external forces were easily conducted along the soft and flexible molecular chains and concentrated on the cross-linking points. It triggered part of dynamic covalent bonds that were weak and brittle and ruptured preferentially.<sup>45</sup> After a wide cleavage of the central C–C bonds of DFMA, the molecular chains of PHMA could be fully stretched before being finally fractured. The rupture of dynamic covalent bonds consumed an amount of energy and suppressed stress concentration, improving strength and modulus greatly. In our previous research, the exchange ability of dynamic covalent bonds and the formation of CF radicals were confirmed by stress-relaxation measurements and electron paramagnetic resonance (EPR) spectroscopy.<sup>42</sup> The force-relaxation behavior attributed to the structural transition at cross-linking points was not observed in PHMA with HDMA. Meanwhile, toughness and elongation were dramatically improved by stretching the released hidden lengths.

According to Figure 2e, in the first loading–unloading cycle, both dissipated energy and energy dissipation ratio of PHMA with DFMA were higher than those of PHMA with HDMA. When at the same strain of 400%, the dissipated energy of PHMA with dynamic covalent bonds increased to 166.0 kJ·m<sup>-3</sup>, 48.9% higher than that of PHMA with HDMA. The toughening material exhibited greater hysteresis loss, promising better toughness and strength. In PHMA with HDMA, the tension energy was dissipated mainly through intermolecular friction, manifested as the elastic aftereffect. Because additional energy was required for the rupture of sacrificial bonds which occurred widely and stretching the released hidden lengths,<sup>2</sup> the dissipated energy of PHMA with DFMA increased dramatically. It is noted that the energy dissipation ratio of PHMA showed a decreasing trend with increasing stretching. A

total of 89.9% of the tension energy dissipated in the loading–unloading cycle at a strain of 25%. It indicated that elasticity only contributed to a small portion of toughness. Meanwhile, under large deformation, the energy dissipation ratio decreased by nearly 30%, and the polymer network exhibited mainly elastic deformation.<sup>46</sup> The competition between the elasticity of the PHMA main skeleton and the strength of temporarily reassociated dynamic covalent bonds determined the hysteresis behavior and recovery ability.

Without relaxation, the tension energy and dissipated energy of PHMA with DFMA in the second loading–unloading cycle decreased significantly. The tension energy in the second cycle remained 67.2% of that in the first cycle at a strain of 25%, while it decreased to only 45.6% at a strain of 600%. Generated radicals from DFSN upon mechanical stimulation could recombine,<sup>41,42</sup> as shown in Figure 1a. The dissociated bonds broke the cross-linking structure, while the reformed new combination repaired the damaged network gradually. However, without relaxation, fewer bonds played a role as the sacrificial bonds in the following loading–unloading cycle, leading to poor toughness and strength.

The residual strain and shape recovery ability of the PHMA network in two loading–unloading cycles are presented in Figure 3, and related data are listed in Tables S1 and S2. The

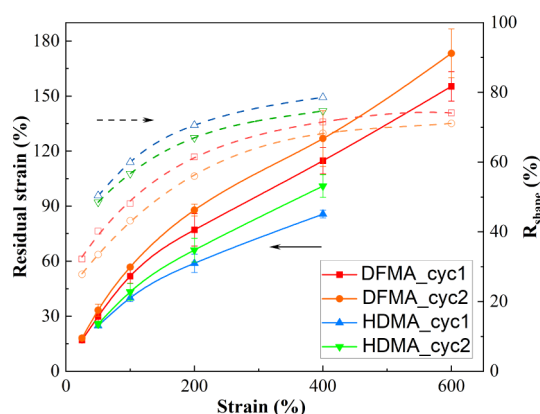


**Figure 3.** Residual strain and shape recovery ability of PHMA with DFMA and HDMA in two loading–unloading cycles,  $R_{\text{shape}}$ : shape recovery ability, and  $R_{\text{shape}} = 1 - \text{residual strain}/\text{tensile strain}$ .

higher  $R_{\text{shape}}$  value represented quicker shape recovery and stronger responsiveness to tension stimulation. In PHMA with HDMA, the cross-linking density was barely changed during tension, which maintained the restriction on the segments' movement and ensured higher elastic resilience. It ensured quicker recovery of PHMA with HDMA both in energy and shape, showing a higher  $R_{\text{energy}}$  value (Tables S1 and S2), smaller residual strain, and higher  $R_{\text{shape}}$  value (Figure 3). Unlike this, the dynamic covalent bonds ruptured gradually when loading, causing continuous damage to the cross-linking structure and a decrease in cross-linking density. Under larger deformation, the decline became even more serious, and the incomplete cross-linking network weakened the restriction on the segments' movement. Thus, the molecular chains slipped easily. The ruptured dynamic covalent bonds could reassociate at newly accessible sites, forming a resistance for recovery. These temporarily reassociated bonds would be ruptured by the elastic contractions from the main skeleton. It caused a slow recovery of PHMA with DFMA in shape and energy.

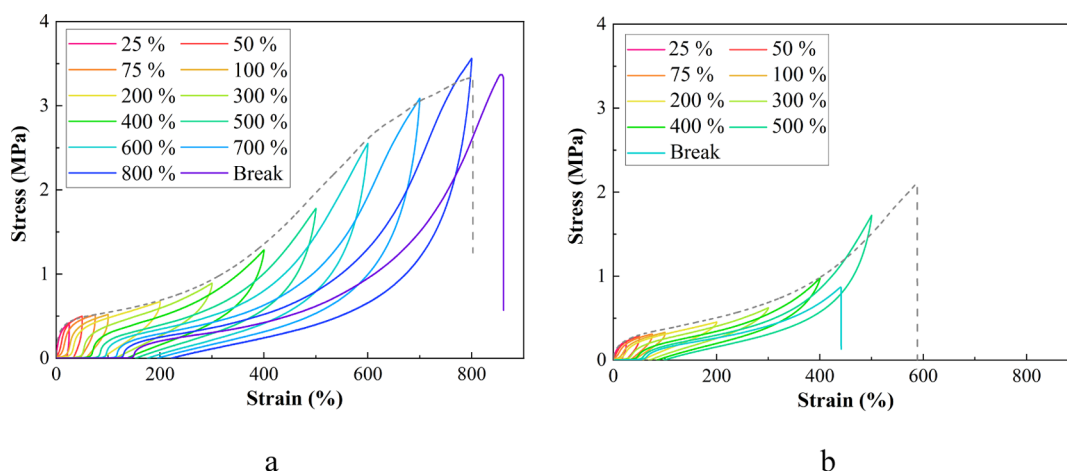


**Figure 4.** Stress–strain curves of PHMA with DFMA (a) and HDMA (b) in continuous loading–unloading cycles. The gray dotted line from the result of a single tension was shown as a reference.

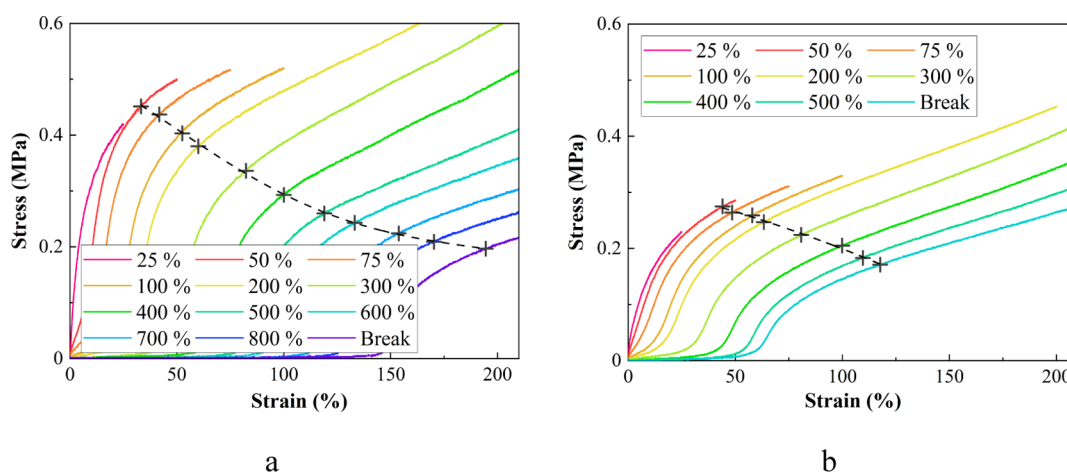


**Figure 5.** Yield points of PHMA with DFMA (a) and HDMA (b) in continuous loading–unloading cycles based on the Considère criterion analysis.<sup>43,44</sup>

**3.2. Mechanical Properties in Continuous Loading–Unloading Cycles.** The stress–strain curves of PHMA cross-linked by DFMA and HDMA in continuous loading–unloading cycles are presented in Figure 4. Compared to PHMA with HDMA, PHMA with DFMA showed greater hysteresis loops, higher modulus, and stronger toughness in all loading–unloading cycles. The yield point of the PHMA soft material in each testing cycle was determined based on the Considère criterion analysis,<sup>43,44</sup> presented in Figure 5, and the corresponding yield stress is listed in Table S3. The higher yield stress and smaller yield strain of PHMA indicated the stronger and tougher properties owing to the introduction of dynamic covalent bonds. The yield stress reduced gradually with each loading–unloading cycle, from 0.46 to 0.20 MPa. The decreasing trend of yield stress in PHMA with DFMA was more significant than that in PHMA with HDMA, which changed from 0.29 to 0.18 MPa. It illustrated that the rupture of dynamic covalent bonds occurred gradually with continuous tension stimulation, and the tension energy was dissipated within every stage of deformation. Two main factors had effects on the yield stress, which were the orientation of the main skeleton and the cross-linking density of the polymer network. Generally, after repeated tension stimulation, the arrangement of segments in the polymer

tended to be oriented from the disordered state for adapting the reciprocating deformation.<sup>47</sup> In PHMA with DFMA, the reduction of cross-linking density was caused by the rupture of the central C–C bonds of DFMA. This effect became stronger because of the rupture of reassociated bonds with continuous tension stimulation. The fractured sacrificial bonds and reorganization of the polymer network broke the cross-linked structure, causing a greater decline in yielding stress.

According to Figure 4a, after continuous loading–unloading cycles, PHMA with DFMA reached a higher value of maximum stress and elongation than the result of a single tension (shown in the gray dotted line). Stress toughening brought higher strength because of the improvement of segment orientation.<sup>47</sup> Under continuous stress, the restriction on segments' movement was relatively weakened owing to the wide rupture of the central C–C bonds of DFMA and the reduction of cross-linking density. The decrease in the degree of cross-linking density effectively reduced the steric hindrance of the molecular chains and improved the mobility of the segments.<sup>46,48</sup> Molecular chains were expected to align easily in the direction of the external force.<sup>2,47,49</sup> The effect of stress-induced orientation improved the mechanical properties.

The PHMA toughening soft material with dynamic covalent bonds showed a remarkable hysteresis loop and mechanical

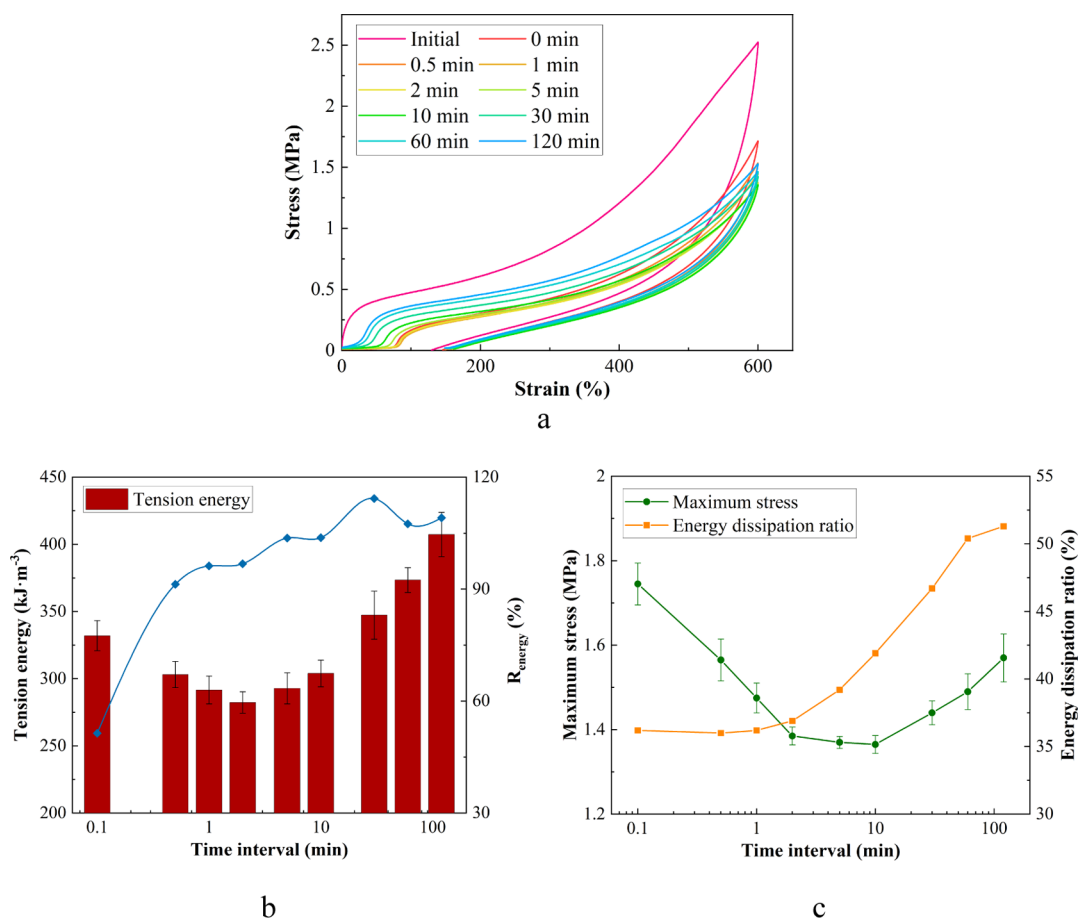


**Figure 6.** Stress–strain curves of PHMA with DFMA in the stretching–relaxation process with different time intervals (a) and tension energy recovery (b) and mechanical performance (c) after relaxation.

**Table 1. Mechanical Properties of PHMA with DFMA in the Stretching–Relaxation Process with Different Time Intervals<sup>a</sup>**

time intervals (min)	stress <sub>max</sub> (MPa)	$W_t$ (kJ·m <sup>-3</sup> )	$R_{\text{energy}}$ (%)	$W_d$ (kJ·m <sup>-3</sup> )	$D_{\text{energy}}$ (%)
initial	2.57 ± 0.07	646.4 ± 25.2		390.3 ± 32.3	60.4
0	1.75 ± 0.05	332.0 ± 11.3	51.4	120.1 ± 5.5	36.2
0.5	1.57 ± 0.05	303.1 ± 9.7	91.3	109.1 ± 7.0	36.0
1	1.48 ± 0.04	291.6 ± 10.4	96.2	105.5 ± 6.4	36.2
2	1.39 ± 0.02	282.4 ± 8.0	96.8	104.1 ± 5.5	36.9
5	1.37 ± 0.01	292.8 ± 11.6	103.7	114.9 ± 7.3	39.2
10	1.37 ± 0.02	303.9 ± 10.0	103.8	127.4 ± 7.9	41.9
30	1.44 ± 0.03	347.4 ± 17.9	114.3	162.1 ± 15.4	46.7
60	1.49 ± 0.04	373.5 ± 9.3	107.5	188.2 ± 15.3	50.4
120	1.57 ± 0.06	407.4 ± 16.5	109.1	208.9 ± 15.7	51.3

<sup>a</sup>Stress<sub>max</sub>: maximum stress in one loading–unloading cycle.  $R_{\text{energy}}$ : energy recovery ability and  $R_{\text{energy}} = W_{t\_cyc(n+1)}/W_{t\_cyc(n)}$ .

enhancement in tension. Here, a possible explanation for the energy dissipation behavior and structure transition in tension was proposed. A brittle and weak cross-linking point was introduced into the flexible polymer network with a DFMA mechanochromic cross-linker via free radical polymerization. It formed a constrained network having segments with different lengths between cross-linking points. Under stress, short-chain segments extended, and their orientation improved immediately. External forces were applied along the molecular chains and concentrated on the weak central C–C bonds of DFMA. It triggered part of dynamic covalent bonds that ruptured preferentially and released the hidden lengths, resulting in higher yield stress and lower cross-linking density than the

polymer with the conventional cross-linker. Then, the rest of the dynamic covalent bonds ruptured gradually during stretching, while the dissociated bonds slipped along the molecular chains and reassociated at newly accessible sites continuously. The reorganization of short-chain segments induced the orientation of the long-chain segments. It effectively improved the strength, toughness, and elongation of the PHMA soft material. Except for intermolecular friction, additional energy was consumed through the rupture of dynamic covalent bonds and stretching the released hidden lengths. Under large deformation, the elastic contractions of the main skeleton were dominant.<sup>50</sup> In small deformation, the elastic contractions became weak. The reassociated DFSN

moieties, as well as the reorganization of the network structure, slowed down the recovery of the main skeleton to its initial state. Incorporating dynamic covalent bonds into PHMA promised excellent mechanical enhancement and energy dissipation capacity of the soft material.

### 3.3. Energy Recovery Ability and Mechanoresponsive Color Evaluation in the Stretching–Relaxation Process.

To investigate the dissociation and reassociation of dynamic covalent bonds, the tensile behavior of PHMA with a series of different time intervals was studied. The hysteresis loops in loading–unloading cycles and energy recovery ability of the polymer in the stretching–relaxation process are shown in Figure 6, and related mechanical properties are summarized in Table 1. PHMA with DFMA had a remarkable hysteresis loop in the first loading–unloading cycle with a dissipated energy of  $646.4 \text{ kJ}\cdot\text{m}^{-3}$ . The hysteresis loops in the successive cycles were much smaller than that of the first cycle, indicating that fewer central C–C bonds of DFMA offered energy dissipation capacity. In the second testing cycle with no relaxation (time interval 0 min), the maximum tensile strength dropped by 68.1%, and the tension energy was only 51.4% than that in the first cycle. The tension energy and dissipated energy continuously decreased in subsequent cycles. They both reached the lowest value in the fifth cycle after a time interval of 2 min. As discussed previously, the cross-linking structure was damaged because of the rupture of dynamic covalent bonds, and reassociated bonds at newly accessible sites slowed down the recovery. After relaxation for 5 min, the  $R_{\text{energy}}$  value reached 103.7%, and then, the mechanical properties recovered as the waiting time increased. Meanwhile, the hysteresis loss curves gradually approached the first cycle. However, the recovery process was time-consuming. After the relaxation for 120 min, the tension energy was only  $407.4 \text{ kJ}\cdot\text{m}^{-3}$ , still 37.0% lower than that in the first cycle, and the tensile strength was 61.1% of the initial strength. After experiencing a large deformation, PHMA cross-linked by DFMA retained a certain residual strain even after relaxation for 5 days.

Under stress, the rupture of the central C–C bonds of DFMA generated reversible and stable pink-colored CF radicals. The more the CF radicals generated, the stronger the pink color could be detected. It allowed us to quantitatively evaluate the energy dissipation by investigating the color change. The photographs of PHMA with DFMA at different strains in the first loading–unloading cycle are shown in Figure 7, and the actual color on the surface are also figured out. The color of PHMA changed from light gray to pink with increasing deformation, which started to appear at the strain around 500%. The toughening polymer showed a clear and distinct pink color at a strain of 600%. In the unloading

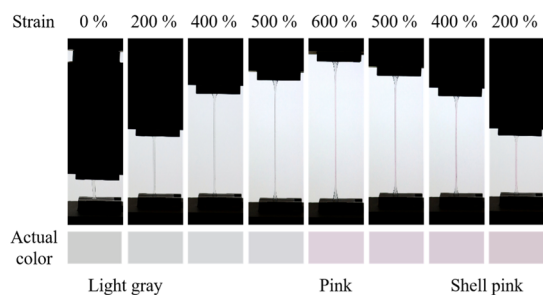


**Figure 7.** Photographs of PHMA with DFMA at different stains in the first loading–unloading cycle and the actual color on the surface.

process, the brightness on the surface was reduced because of increasing thickness. The color became darker and appeared shell pink eventually.

According to the hysteresis analysis, external forces were applied along the molecular chain easily, and extended soft segments led to a stress concentration on the weak central C–C bonds of DFMA. Part of dynamic covalent bonds ruptured preferentially before a wide cleavage of these bonds. However, the generated pink color under small deformation was too weak to be detected by our naked eyes. For a quantitative evaluation of the color change, the red channel intensity distributions on the surface of the sample extracted from digital images in the first loading–unloading cycle are shown in Figure 8. The increased intensity during stretching indicated a wide cleavage of dynamic covalent bonds. For a better comparison of the average value, the red channel intensities on the central axis of the tensile direction are also shown in Figure 9. It was noted that at small deformation, the red channel intensity barely increased. On the 3D color map, red channel intensity and its distribution increased greatly when the deformation was greater than 400%. This result was consistent with our previous study.<sup>42</sup> Through EPR measurement, it was found that the dissociation ratio of dynamic covalent bonds increased negligibly under small deformation. The red channel intensity reached the highest value and covered the widest area at a strain of 600%. The intensity distributions were uniform both on the surface and on the tensile direction, and no concentration was observed. The broad intensity distribution under large deformation indicated that the rupture of dynamic covalent bonds occurred evenly throughout the polymer and suppressed stress concentration effectively. Besides, according to Figure 9, the average intensity decreased during unloading, indicating the reassociation of ruptured bonds. The intensities during unloading were stronger than those at the same strain in loading, indicating that only part of the dissociated bonds reformed new combination. This analysis method proved that PHMA cross-linked by DFMA showed responsiveness to tension stimulation and had extraordinary energy dissipation capacity.

To further study the dissociation of dynamic covalent bonds, the RGB value changes on the surface of PHMA cross-linked by DFMA in the stretching–relaxation process were investigated. According to experimental observation, color changes were much lighter in the successive cycles compared to the color observed in the first cycle. When being stimulated by large deformation for the first time, more bonds were ruptured, contributing to a great hysteresis loop in energy and distinct pink color in visual. The mechanoresponsive color changes with different time intervals are shown in Figure S1. The average RGB values, which were obtained from white-balanced digital images, changed within narrow ranges except for the first cycle. According to Figure S1, when the polymer had the strongest pink color, the three primary color channel intensities reached the highest in red, relatively low in green, and medium in blue. However, it was noted that RGB values changed linearly with strain both in the loading and unloading processes, except for the first loading–unloading cycle. The color-changing trends to strain in the successive cycles with different time intervals did not approach that from the first testing cycle. Such changes also did not match the forecast from the hysteresis analysis and tension energy recovery results after relaxation. We considered that this change was due to the change in chromaticity caused by the sample thickness during

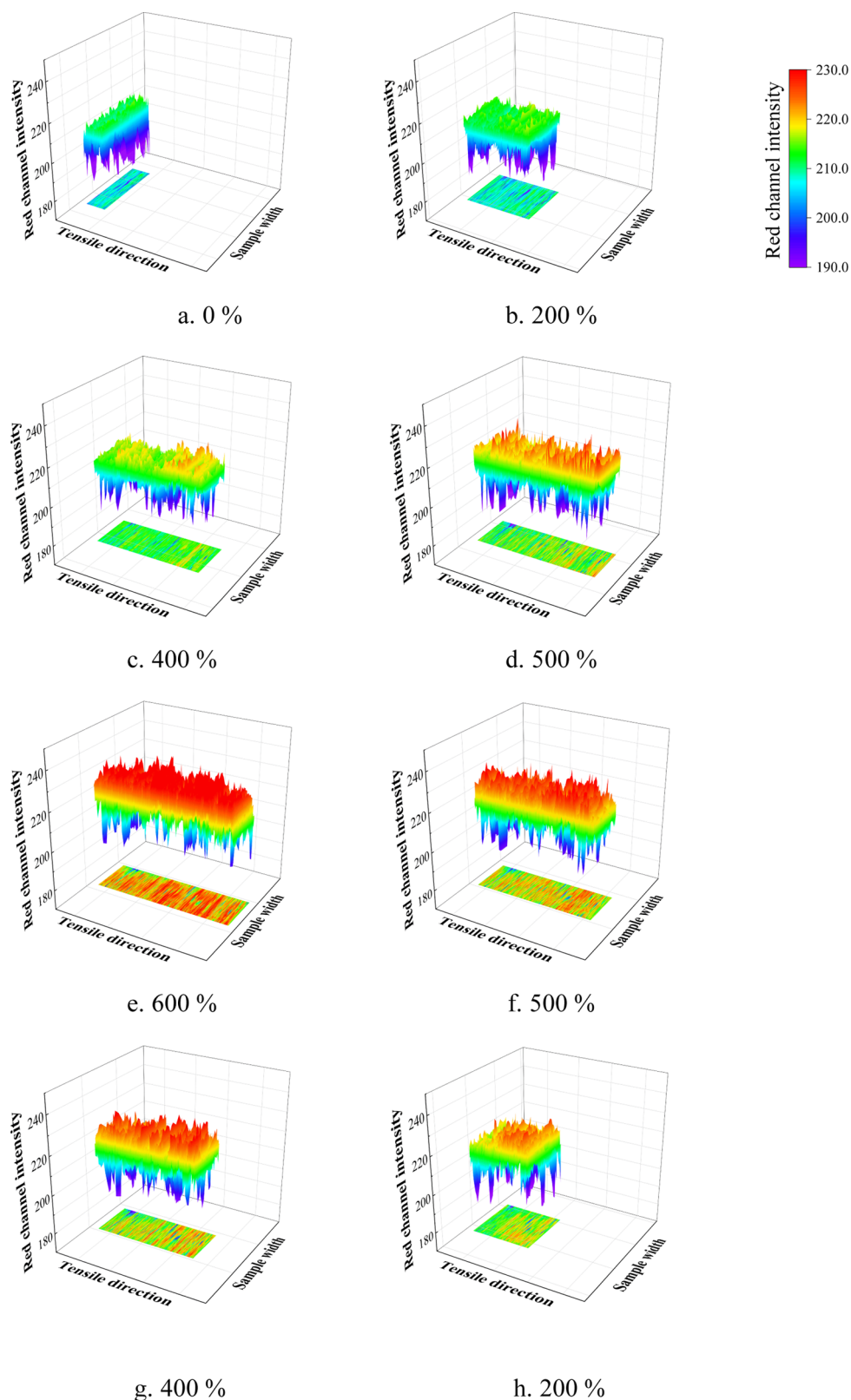


**Figure 8.** 3D color maps of red channel intensity distribution on the surface of PHMA with DFMA in the first loading–unloading cycle at different strains (X-axis: sample length on the tensile direction and Y-axis: sample width).

the loading–unloading cycle. Compared to strain, the RGB channel intensities showed more relevance to stress.

The functions of mechanoresponsive color change to the stress of PHMA cross-linked by DFMA during loading with

different relaxation time intervals are presented in Figure 10. In the unloading process, the ruptured dynamic covalent bonds could not reassociate immediately, so the detected color could not represent the actual stress changes in the polymer. Also, it

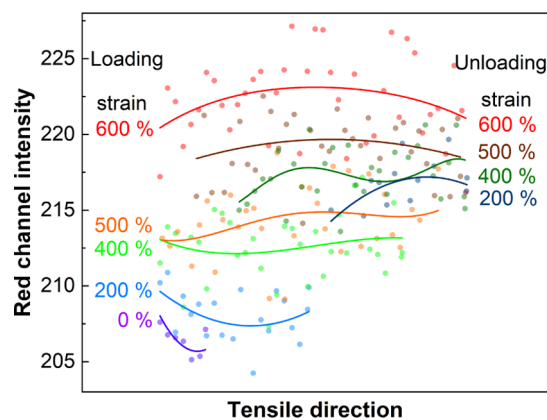


**Figure 9.** Red channel intensities of PHMA with DFMA on the central axis of the tensile direction at different strains. The fitting lines represented the average value in the center of samples (X-axis: sample length on the tensile direction).

was the same situation to the data obtained from 0 and 0.5 min tests owing to the slow recovery. Thus, RGB values obtained from the abovementioned processes were excluded for fitting calculation. According to the fitting results, RGB channel intensities showed a strong dependence on the stress in tension. Coefficients of determination ( $R^2$ ) to all three primary

color channels were higher than 0.90, ensuring excellent credibility. For the red channel, the intensity increased rapidly when stress was greater than 1.5 MPa. Besides, the intensities of the green and blue channels reached a maximum value at strains of 1.3 and 1.6 MPa, respectively. The color simulation based on the fitting results of the average RGB are presented in **Figure 11**. The simulated colors were close to the observed

Stress (MPa)	0	0.5	1.0	1.5	2.0	2.5
Color simulation						
RGB	(207.1, 207.0, 205.3)	(211.7, 213.6, 214.9)	(214.1, 218.6, 220.3)	(215.0, 219.0, 222.3)	(216.5, 214.9, 222.0)	(221.9, 209.7, 220.3)

**Figure 11.** Color simulation based on the fitting results of average RGB to stress.

actual colors, which are shown in **Figure 7**. The pink color started to appear at the stress in the range of 1.5–2.0 MPa. Such a stress range corresponded to the strain from 454 to 525% in the first loading–unloading cycle. The result was consistent with the experimental observation. By analyzing the mechanoresponsive color changes, we could evaluate the stress in the PHMA toughening polymer.

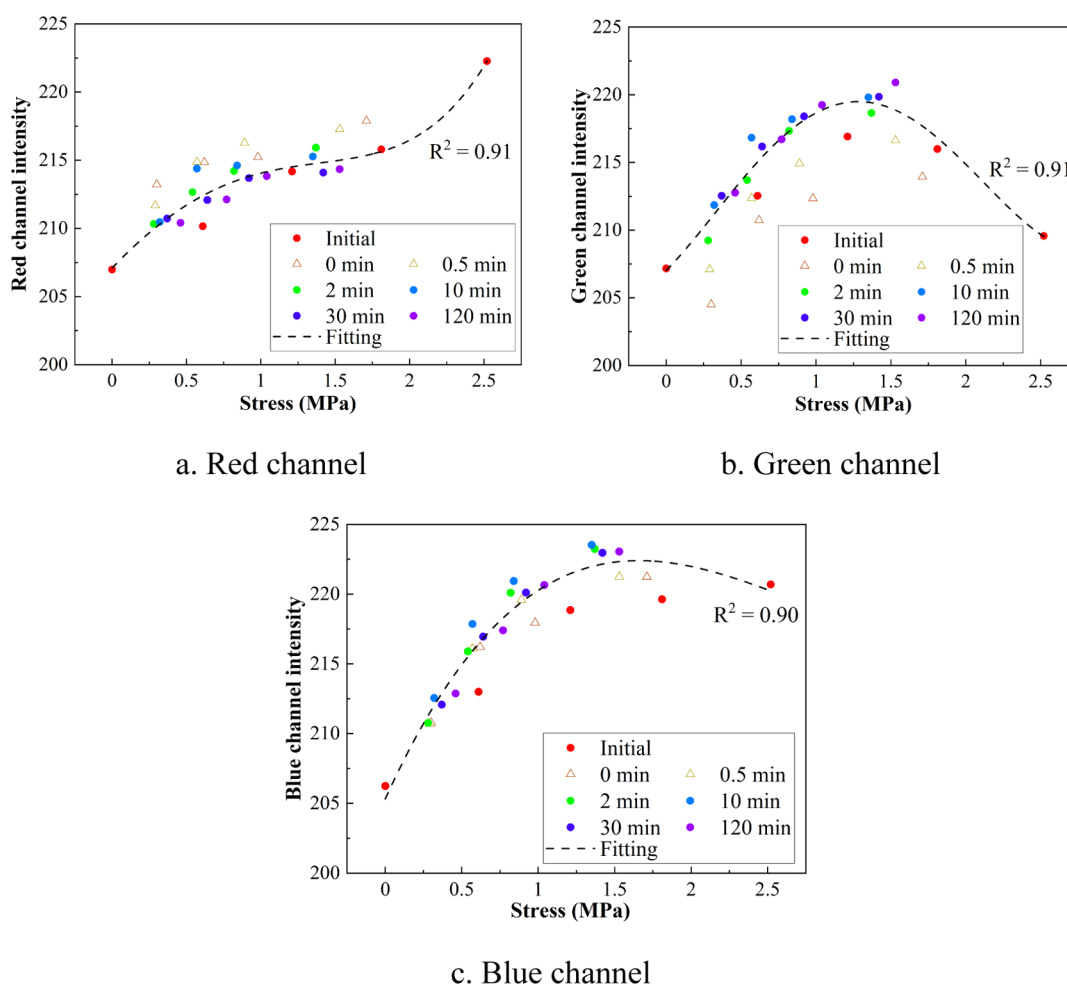


**Figure 10.** Fitting curves of mechanoresponsive color change to the stress of PHMA with DFMA during loading with different relaxation time intervals. The RGB values obtained from 0 and 0.5 min tests were shown as references.

## 4. CONCLUSIONS

A rigid and brittle cross-linked structure was introduced into the flexible PHMA polymer network by the mechanochromic cross-linker DFMA via radical polymerization. Compared to PHMA with the conventional cross-linker HDMA, PHMA with the DFMA toughening polymer showed a remarkable hysteresis loop with an energy dissipation ratio of up to 62.2% at a strain of 600% and mechanical enhancement in tension. The breaking stress of the toughening polymer was up to 3.29 MPa that was 1.5 times higher, with a fracture energy of 1278.1 kJ·m<sup>-3</sup> increased by 289%, while the maximum elongation at break reaching 810.2% increased by 151%. In the PHMA polymer, the dissociation and reassociation of dynamic covalent bonds was the key element for toughening and energy dissipation. The wide cleavage of the central C–C bonds of DFMA and stretching the hidden lengths consumed the amount of energy and suppressed stress concentration, increasing strength and toughness greatly. Dynamic covalent bonds ruptured gradually during stretching, while the dissociated bonds slipped along the molecular chains and reassociated at newly accessible sites continuously. The mobility of segments was improved because of the failure of the cross-linking structure triggered by the rupture of dynamic covalent bonds. The reassociation of dynamic covalent bonds and the reorganization of the network structure slowed down the recovery of the polymer to its initial state.

With the aid of digital image analysis, the generated reversible and detectable pink color was quantitatively evaluated. When being stimulated by large deformation for the first time, more central C–C bonds of DFMA were ruptured, contributing to a great hysteresis loop in energy and distinct pink color in visual. The color of PHMA changed from light gray to pink with increasing deformation and faded during unloading. The broad and uniform distribution of red channel intensity detected on the surface under large deformation confirmed that the rupture of dynamic covalent bonds occurred evenly throughout the polymer and suppressed stress concentration effectively during stretching. The mechanoresponsive color showed a strong dependence on stress. According to the fitting results, the pink color started to appear at the stress in the range of 1.5–2.0 MPa, which was consistent with the experimental observation. The incorporation of DFMA promised enhanced mechanical properties and noncontact stress detection ability of the PHMA soft material. By exploring the correlations between the tension stimulation, energy dissipation, and mechanoresponsive color change, it is expected to promote further development of mechanochromic soft polymer materials.

## ■ ASSOCIATED CONTENT

### SI Supporting Information

The Supporting Information is available free of charge at <https://pubs.acs.org/doi/10.1021/acs.macromol.0c01770>.

Energy dissipation and tensile performance of PHMA with DFMA in the first and second loading–unloading cycles; energy dissipation and tensile performance of PHMA with HDMA in the first and second loading–unloading cycles; yield stress of PHMA with DFMA and HDMA in continuous loading–unloading cycles; and RGB intensities to stress and strain of PHMA with DFMA in the stretching–relaxation process with different time intervals (PDF)

## ■ AUTHOR INFORMATION

### Corresponding Author

**Hiroshi Ito** – Research Center for GREEN Materials & Advanced Processing and Department of Organic Materials Science, Graduate School of Organic Materials Science, Yamagata University, Yonezawa, Yamagata 992-8510, Japan; [orcid.org/0000-0001-8432-8457](https://orcid.org/0000-0001-8432-8457); Email: [ihiroshi@yz.yamagata-u.ac.jp](mailto:ihiroshi@yz.yamagata-u.ac.jp)

### Authors

**Yuchen Mao** – Research Center for GREEN Materials & Advanced Processing, Yamagata University, Yonezawa, Yamagata 992-8510, Japan; [orcid.org/0000-0002-6797-6038](https://orcid.org/0000-0002-6797-6038)

**Yuto Kubota** – Department of Systems Innovation, Faculty of Engineering, Yamagata University, Yonezawa, Yamagata 992-8510, Japan

**Takashi Kurose** – Research Center for GREEN Materials & Advanced Processing, Yamagata University, Yonezawa, Yamagata 992-8510, Japan

**Akira Ishigami** – Research Center for GREEN Materials & Advanced Processing and Department of Organic Materials Science, Graduate School of Organic Materials Science, Yamagata University, Yonezawa, Yamagata 992-8510, Japan

**Kota Seshimo** – Department of Chemical Science and Engineering, Tokyo Institute of Technology, Meguro-ku, Tokyo 152-8550, Japan

**Daisuke Aoki** – Department of Chemical Science and Engineering, Tokyo Institute of Technology, Meguro-ku, Tokyo 152-8550, Japan; [orcid.org/0000-0002-7272-0643](https://orcid.org/0000-0002-7272-0643)

**Hideyuki Otsuka** – Department of Chemical Science and Engineering, Tokyo Institute of Technology, Meguro-ku, Tokyo 152-8550, Japan; [orcid.org/0000-0002-1512-671X](https://orcid.org/0000-0002-1512-671X)

Complete contact information is available at:

<https://pubs.acs.org/10.1021/acs.macromol.0c01770>

### Notes

The authors declare no competing financial interest.

## ■ ACKNOWLEDGMENTS

This work was financially supported by JST CREST grant JPMJCR1991 (Japan).

## ■ REFERENCES

- (1) Xiao, L.; Huang, J.; Wang, Y.; Chen, J.; Liu, Z.; Nie, X. Tung Oil-Based Modifier Toughening Epoxy Resin by Sacrificial Bonds. *ACS Sustainable Chem. Eng.* **2019**, *7*, 17344–17353.
- (2) Huang, J.; Zhang, L.; Tang, Z.; Guo, B. Bioinspired engineering of sacrificial bonds into rubber networks towards high-performance and functional elastomers. *Compos. Commun.* **2018**, *8*, 65–73.
- (3) Grossman, M.; Bouville, F.; Erni, F.; Masania, K.; Libanori, R.; Studart, A. R. Mineral Nano-Interconnectivity Stiffens and Toughens Nacre-like Composite Materials. *Adv. Mater.* **2017**, *29*, 1605039.
- (4) Li, C.; Wang, Y.; Yuan, Z.; Ye, L. Construction of sacrificial bonds and hybrid networks in EPDM rubber towards mechanical performance enhancement. *Appl. Surf. Sci.* **2019**, *484*, 616–627.
- (5) Lv, C.; Wang, J.; Li, Z.; Zhao, K.; Zheng, J. Degradable, reprocessable, self-healing PDMS/CNTs nanocomposite elastomers with high stretchability and toughness based on novel dual-dynamic covalent sacrificial system. *Composites, Part B* **2019**, *177*, 107270.
- (6) Chen, H.; Yang, F.; Chen, Q.; Zheng, J. A Novel Design of Multi-Mechanoresponsive and Mechanically Strong Hydrogels. *Adv. Mater.* **2017**, *29*, 1606900.

- (7) Haque, M. A.; Kurokawa, T.; Gong, J. P. Super tough double network hydrogels and their application as biomaterials. *Polymer* **2012**, *53*, 1805–1822.
- (8) Neal, J. A.; Mozhdzhi, D.; Guan, Z. Enhancing mechanical performance of a covalent self-healing material by sacrificial noncovalent bonds. *J. Am. Chem. Soc.* **2015**, *137*, 4846–4850.
- (9) Liu, Y.; Tang, Z.; Wu, S.; Guo, B. Integrating Sacrificial Bonds into Dynamic Covalent Networks toward Mechanically Robust and Malleable Elastomers. *ACS Macro Lett.* **2019**, *8*, 193–199.
- (10) Henderson, K. J.; Zhou, T. C.; Otim, K. J.; Shull, K. R. Ionically Cross-Linked Triblock Copolymer Hydrogels with High Strength. *Macromolecules* **2010**, *43*, 6193–6201.
- (11) Zhou, X.; Guo, B.; Zhang, L.; Hu, G.-H. Progress in bio-inspired sacrificial bonds in artificial polymeric materials. *Chem. Soc. Rev.* **2017**, *46*, 6301–6329.
- (12) Maeda, T.; Otsuka, H.; Takahara, A. Dynamic covalent polymers: Reorganizable polymers with dynamic covalent bonds. *Prog. Polym. Sci.* **2009**, *34*, 581–604.
- (13) Nakajima, T.; Kurokawa, T.; Ahmed, S.; Wu, W.-l.; Gong, J. P. Characterization of Internal Fracture Process of Double Network Hydrogels under Uniaxial Elongation. *Soft Matter* **2013**, *9*, 1955–1966.
- (14) Gong, J. P. Materials both Tough and Soft. *Science* **2014**, *344*, 161–162.
- (15) Peterson, G. I.; Larsen, M. B.; Ganter, M. A.; Storti, D. W.; Boydston, A. J. 3D-printed mechanochromic materials. *ACS Appl. Mater. Interfaces* **2015**, *7*, 577–583.
- (16) Cellini, F.; Zhou, L.; Khapli, S.; Peterson, S. D.; Porfiri, M. Large deformations and fluorescence response of mechanochromic polyurethane sensors. *Mech. Mater.* **2016**, *93*, 145–162.
- (17) Chen, Y.; Spiering, A. J. H.; Karthikeyan, S.; Peters, G. W. M.; Meijer, E. W.; Sijbesma, R. P. Mechanically induced chemiluminescence from polymers incorporating a 1,2-dioxetane unit in the main chain. *Nat. Chem.* **2012**, *4*, 559–562.
- (18) Stratigaki, M.; Göstl, R. Methods for Exerting and Sensing Force in Polymer Materials Using Mechanophores. *Chempluschem* **2020**, *85*, 1095.
- (19) Davis, D. A.; Hamilton, A.; Yang, J.; Cremer, L. D.; Van Gough, D.; Potisek, S. L.; Ong, M. T.; Braun, P. V.; Martínez, T. J.; White, S. R.; Moore, J. S.; Sottos, N. R. Force-induced activation of covalent bonds in mechanoresponsive polymeric materials. *Nature* **2009**, *459*, 68–72.
- (20) Celestine, A.-D. N.; Beiermann, B. A.; May, P. A.; Moore, J. S.; Sottos, N. R.; White, S. R. Fracture-induced activation in mechanophore-linked, rubber toughened PMMA. *Polymer* **2014**, *55*, 4164–4171.
- (21) Degen, C. M.; May, P. A.; Moore, J. S.; White, S. R.; Sottos, N. R. Time-Dependent Mechanochemical Response of SP-Cross-Linked PMMA. *Macromolecules* **2013**, *46*, 8917–8921.
- (22) Celestine, A.-D. N.; Sottos, N. R.; White, S. R. Strain and stress mapping by mechanochemical activation of spiropyran in poly(methyl methacrylate). *Strain* **2019**, *55*, No. e12310.
- (23) Kim, T. A.; Lamuta, C.; Kim, H.; Leal, C.; Sottos, N. R. Interfacial Force-Focusing Effect in Mechanophore-Linked Nanocomposites. *Adv. Sci.* **2020**, *7*, 1903464.
- (24) Sulkanen, A. R.; Sung, J.; Robb, M. J.; Moore, J. S.; Sottos, N. R.; Liu, G.-y. Spatially Selective and Density-Controlled Activation of Interfacial Mechanophores. *J. Am. Chem. Soc.* **2019**, *141*, 4080–4085.
- (25) Imato, K.; Irie, A.; Kosuge, T.; Ohishi, T.; Nishihara, M.; Takahara, A.; Otsuka, H. Mechanophores with a reversible radical system and freezing-induced mechanochemistry in polymer solutions and gels. *Angew. Chem., Int. Ed.* **2015**, *54*, 6168–6172.
- (26) Imato, K.; Kanehara, T.; Ohishi, T.; Nishihara, M.; Yajima, H.; Ito, M.; Takahara, A.; Otsuka, H. Mechanochromic Dynamic Covalent Elastomers: Quantitative Stress Evaluation and Autonomous Recovery. *ACS Macro Lett.* **2015**, *4*, 1307–1311.
- (27) Imato, K.; Kanehara, T.; Nojima, S.; Ohishi, T.; Higaki, Y.; Takahara, A.; Otsuka, H. Repeatable mechanochemical activation of dynamic covalent bonds in thermoplastic elastomers. *Chem. Commun.* **2016**, *52*, 10482–10485.
- (28) Kosuge, T.; Imato, K.; Goseki, R.; Otsuka, H. Polymer-Inorganic Composites with Dynamic Covalent Mechanochromophore. *Macromolecules* **2016**, *49*, 5903–5911.
- (29) Oka, H.; Imato, K.; Sato, T.; Ohishi, T.; Goseki, R.; Otsuka, H. Enhancing Mechanochemical Activation in the Bulk State by Designing Polymer Architectures. *ACS Macro Lett.* **2016**, *5*, 1124–1127.
- (30) Imato, K.; Natterodt, J. C.; Sapkota, J.; Goseki, R.; Weder, C.; Takahara, A.; Otsuka, H. Dynamic covalent diarylbibenzofuranone-modified nanocellulose: mechanochromic behaviour and application in self-healing polymer composites. *Polym. Chem.* **2017**, *8*, 2115–2122.
- (31) Imato, K.; Otsuka, H. Reorganizable and stimuli-responsive polymers based on dynamic carbon-carbon linkages in diarylbibenzofuranones. *Polymer* **2018**, *137*, 395–413.
- (32) Ishizuki, K.; Oka, H.; Aoki, D.; Goseki, R.; Otsuka, H. Mechanochromic Polymers That Turn Green Upon the Dissociation of Diarylbibenzothiophenonyl: The Missing Piece toward Rainbow Mechanochromism. *Chem.—Eur. J.* **2018**, *24*, 3170–3173.
- (33) Kosuge, T.; Zhu, X.; Lau, V. M.; Aoki, D.; Martinez, T. J.; Moore, J. S.; Otsuka, H. Multicolor Mechanochromism of a Polymer/Silica Composite with Dual Distinct Mechanophores. *J. Am. Chem. Soc.* **2019**, *141*, 1898–1902.
- (34) Lu, Y.; Aoki, D.; Sawada, J.; Kosuge, T.; Sogawa, H.; Otsuka, H.; Takata, T. Visualization of the slide-ring effect: a study on movable cross-linking points using mechanochromism. *Chem. Commun.* **2020**, *56*, 3361–3364.
- (35) Sumi, T.; Goseki, R.; Otsuka, H. Tetraarylsuccinonitriles as mechanochromophores to generate highly stable luminescent carbon-centered radicals. *Chem. Commun.* **2017**, *53*, 11885–11888.
- (36) Ishizuki, K.; Aoki, D.; Goseki, R.; Otsuka, H. Multicolor Mechanochromic Polymer Blends That Can Discriminate between Stretching and Grinding. *ACS Macro Lett.* **2018**, *7*, 556–560.
- (37) Kato, S.; Ishizuki, K.; Aoki, D.; Goseki, R.; Otsuka, H. Freezing-Induced Mechanoluminescence of Polymer Gels. *ACS Macro Lett.* **2018**, *7*, 1087–1091.
- (38) Kato, S.; Aoki, D.; Otsuka, H. Introducing static cross-linking points into dynamic covalent polymer gels that display freezing-induced mechanofluorescence: enhanced force transmission efficiency and stability. *Polym. Chem.* **2019**, *10*, 2636–2640.
- (39) Hoshino, F.; Kosuge, T.; Aoki, D.; Otsuka, H. Mechano-fluorescent polymer/silsesquioxane composites based on tetraarylsuccinonitrile. *Mater. Chem. Front.* **2019**, *3*, 2681–2685.
- (40) Kawasaki, K.; Aoki, D.; Otsuka, H. Diarylbibenzofuranones as Substituent-Tunable Mechanochromophores and Their Application in Mechanochromic Polymers. *Macromol. Rapid Commun.* **2020**, *41*, 1900460.
- (41) Sakai, H.; Sumi, T.; Aoki, D.; Goseki, R.; Otsuka, H. Thermally Stable Radical-Type Mechanochromic Polymers Based on Difluoroenylsuccinonitrile. *ACS Macro Lett.* **2018**, *7*, 1359–1363.
- (42) Sakai, H.; Aoki, D.; Seshimo, K.; Mayumi, K.; Nishitsuji, S.; Kurose, T.; Ito, H.; Otsuka, H. Visualization and Quantitative Evaluation of Toughening Polymer Networks by a Sacrificial Dynamic Cross-Linker with Mechanochromic Properties. *ACS Macro Lett.* **2020**, *9*, 1108–1113.
- (43) Crist, B.; Metaxas, C. Neck propagation in polyethylene. *J. Polym. Sci., Part B: Polym. Phys.* **2004**, *42*, 2081–2091.
- (44) Hillmansen, S.; Haward, R. N. Adiabatic failure in polyethylene. *Polymer* **2001**, *42*, 9301–9312.
- (45) Nakajima, T. Generalization of the sacrificial bond principle for gel and elastomer toughening. *Polym. J.* **2017**, *49*, 477–485.
- (46) Chen, Y.; Tang, Z.; Liu, Y.; Wu, S.; Guo, B. Mechanically Robust, Self-Healable, and Reprocessable Elastomers Enabled by Dynamic Dual Cross-Links. *Macromolecules* **2019**, *52*, 3805–3812.
- (47) Wang, J.; Geng, X.; Wang, W.; Zhang, L.; Zhao, X.; Nishi, T. Nitrile rubber/sliding graft copolymer damping material with

significantly improved strength and damping performance. *J. Appl. Polym. Sci.* **2019**, *136*, 47188.

(48) Ducrot, E.; Chen, Y.; Bulters, M.; Sijbesma, R. P.; Creton, C. Toughening elastomers with sacrificial bonds and watching them break. *Science* **2014**, *344*, 186–189.

(49) Bokobza, L.; Erman, B. A Theoretical and Experimental Study of Filler Effect on Stress-Deformation-Segmental Orientation Relations for Poly(dimethylsiloxane) Networks. *Macromolecules* **2000**, *23*, 8858–8864.

(50) Luo, M.-C.; Zeng, J.; Xie, Z.-T.; Wei, L.-Y.; Huang, G.; Wu, J. Impact of hydrogen bonds dynamics on mechanical behavior of supramolecular elastomer. *Polymer* **2016**, *105*, 221–226.